THE STRUCTURAL DESIGN OF TALL AND SPECIAL BUILDINGS
Struct. Design Tall Spec. Build. **22**, 217–234 (2013)
Published online 2 December 2010 in Wiley Online Library (wileyonlinelibrary.com). DOI: 10.1002/tal.680

A simple approximate method for free vibration analysis of framed tube structures

R. Kamgar and R. Rahgozar*,†

Department of Civil Engineering, Shahid Bahonar University of Kerman, Kerman, Iran

SUMMARY

A simple approximate method is developed for determining natural frequency of tall buildings. Timoshenko's beam model, which considers the influence of shear and flexural deformation, was used in modelling framed tube structures. In this paper, natural frequency and mode shape of framed tube structures were calculated based on the flexural and shear rigidities along with the effects of rotational inertia. Dynamic model of Timoshenko's beam can be obtained by writing equilibrium equations of forces acting on an infinite element. The solution of the dynamic model was obtained by first applying the separation of variables to time and space, followed by the assumption of harmonic motion in time, the steady state eigen system was obtained. Natural frequencies of framed tube structures were calculated by solving the eigenproblem. A numerical example has been presented to demonstrate the ease of application and accuracy of the proposed method. The structure's fundamental frequency was computed using ETABS V9.0.0 (Computer and Structures, Berkeley, California, USA) and compared with the result obtained from proposed method, which shows that the percentage of error was low and acceptable. The proposed method can be adopted as an alternative procedure to evaluate the natural frequency of framed tube in the preliminary stages of structural design. Copyright © 2010 John Wiley & Sons, Ltd.

Received 25 January 2010; Revised 14 August 2010; Accepted 13 September 2010

KEY WORDS: free vibration; framed tube; mode shapes; Timoshenko's beam

1. INTRODUCTION

Free vibration analysis plays an important role in structural design of tall buildings, especially the first mode shape because it is the dominant shape in response to wind- and earthquake-induced vibrations in tall buildings. Therefore, it is important to investigate the methods that used to compute natural frequencies and mode shapes of tall buildings. Many researchers in structural engineering have developed methods to obtain accurate theoretical results for the free vibration analysis of tall buildings in past decades. Wang (1996a) obtained a formula directly from the fourth-order Sturm–Liouville differential equations for calculating the natural frequencies of tube-in-tube tall buildings. The variation principle is adopted to derive the fourth-order Sturm–Liouville differential equation and corresponding conditions at the end points. Wang (1996b) soon extended his work to modify the ordinary differential equation solver program to calculate a numerical solution of eigenvalues for free vibration analysis of tube-in-tube tall buildings. An effective approach based on the classical power series method (i.e. method of Frobenius) for solving ordinary differential equations having variable coefficients has widely been applied to solve similar complicated vibration problems. Fung and Yau (2001) used power series method to express the homogeneous solution in calculating the vibration frequencies of a rotating flexible arm carrying a moving mass. Lee (2007) developed a power series solution in obtaining the natural frequencies of tube-in-tube tall buildings. In his work, by reducing partial differential equation of motion to an ordinary differential equation with variable coefficients on the assumption

*Correspondence to: R. Rahgozar, Department of Civil Engineering, University of Kerman, PO. Box 76135-1893, Kerman, Iran.
†E-mail: rahgozar@mail.uk.ac.ir

that the transverse displacement is a harmonic vibration, a power series solution that represents the mode shape function of tube-in-tube tall buildings was derived. Dym and Williams (2007) used two beam models for estimating fundamental frequencies of tall buildings. The models included the coupled two beam model and Timoshenko's beam model. In their work, it was established that the fundamental frequency of tall buildings vary inversely with the building's height. In comparison of the two beam models, it was concluded that Timoshenko's model is appropriate for describing the behaviour of shear wall buildings, while the coupled two-beam model is better suited for shear wall frame buildings.

Kuang and Ng (2004) used matrix method to determine frequencies of coupled vibration in tall building structures. In their work, based on the continuum model and D'Alembert's principle, the governing equation of motion and the corresponding eigenvalue problem were derived, and by applying the Galerkin technique, a general solution method was proposed for coupled vibration analysis of general tall building structures. Free vibration analysis is presented for asymmetric plan frame structures by Kuang and Ng (2009). The analysis includes the frequency and mode shape determinations for the coupled lateral deflection due to the lateral shear deformation and torsional rotation due to St Venant torsion deformation of the structures. Swaddiwudhipong *et al*. (2002) studied on effects of axial deformation and axial force on vibration characteristic of tall buildings. In their work, a tall building composed of frames and shear walls coupled together was idealized as a shear flexure cantilever through the continuum approach. The effects of axial deformation as well as axial forces in the frames were considered and incorporated in the governing equation. Li *et al*. (2002) used differential equations for free vibration analysis of tall cantilevered structures with variable cross-section subjected to various axial loads. Selecting suitable expressions for mass and stiffness distributions as well as for the axial forces acting on tall buildings, the differential equations were reduced to Bessel equations or ordinary equations with constant coefficients. Kaviani *et al*. (2008) used sandwich beam models for determining the natural periods of multi-storey buildings subjected to earthquake. These systems were replaced by a cantilevered Timoshenko or a sandwich beam with varying cross-section. Three kinds of stiffness, including the global bending stiffness, the local bending stiffness and the shear stiffness, were used in modelling tall buildings for vibrational analyzing. Yavari *et al*. (2000) found an efficient solution to the problem of beams bending under singular loading conditions and having various jump discontinuities. In singular loading conditions, they present a theorem by which the equivalent distributed force of a general class of singular loading conditions, and also, they found that when beams have jump discontinuities the form of governing differential equations changes, and they found the governing differential equations in the space of generalized functions. They shown that for Euler–Bernoulli beams with jump discontinuities, the operator of the differential equations remain unchanged, only the force term changes, but for Timoshenko beams with jump discontinuities, in addition to changes in the force terms, the operator of one the governing differential equations changes. It has been pointed out by Dym and Williams (2007) that the natural or fundamental frequency is inversely proportional to the square of that building's height, and in this paper, this fact can be shown when roots of the characteristic equation change by changing the height of building while other properties of the building are constant. By this work, this fact has been shown that by giving information about an specified building, the first root was obtained from characteristic equations of first, second or third states of Equations (26–28), but by increasing the height of the building while the other properties of the building are constant, first root was obtained from first state while by decreasing the height of the building while the other properties of the building are constant, first root was obtained from second or third states of Equations (26–28). The analytical solution of the proposed method versus approximating existing solutions, e.g. power series solution that has been used by Lee (2007) to obtain first natural frequency and so on, is one of the other pro points of this paper. Making three domains and so far, making relevant characteristic equation in each domain are other pro points.

In this paper, the Timoshenko beam model along with the influence of rotational moment of inertia, shear and flexural deformation and assumption of harmonic motion have been used. The partial differential equation is reduced to an ordinary fourth-order differential equation with constant coefficients. This equation is solved over a specified interval by applying appropriate boundary equations. Numerical example for a framed tube structure has been carried out to show the accuracy of the

DOI: 10.1002/tal

proposed method. The results of ETABS V9.0.0 (Computer and Structures, Berkeley, California, USA) are compared with the proposed method.

2. PROGRAMME FORMULATION AND SOLUTION

Consider a framed tube structure as a continuous beam with flexural rigidity $EI(x)$, shear rigidity $K(x)$ $A(x)G$, mass per unit height $m(x)$, rotational moment of inertia $m_I(x)$, dynamic displacement $y(x, t)$ in y-axis direction that is subjected to dynamic lateral loading $p(x, t)$ along the structure's height L as shown in Figure 1.

In order to establish the governing differential equation of motion for this beam, an infinitesimal element of the beam with length dx is under equilibrium with general dynamic loading $p(x, t)$ in the lateral direction as shown in Figure 2. The inertial force (f_I) is equal to $m(x)(\partial^2 y / \partial t^2)dx$. Equilibrium conditions can be applied to the continuum element in vertical direction as shown in Figure 2 using D'Alembert's principle, and by considering free vibration, i.e. $p(x, t) = 0$, one can obtain as follows:

$$\frac{\partial V(x)}{\partial x} + m(x)\frac{\partial^2 y}{\partial t^2} = 0 \tag{1}$$

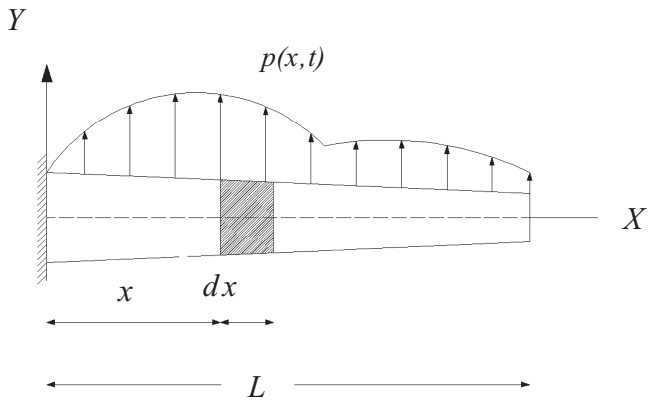

Figure 1. A tall building model with variable cross-section.

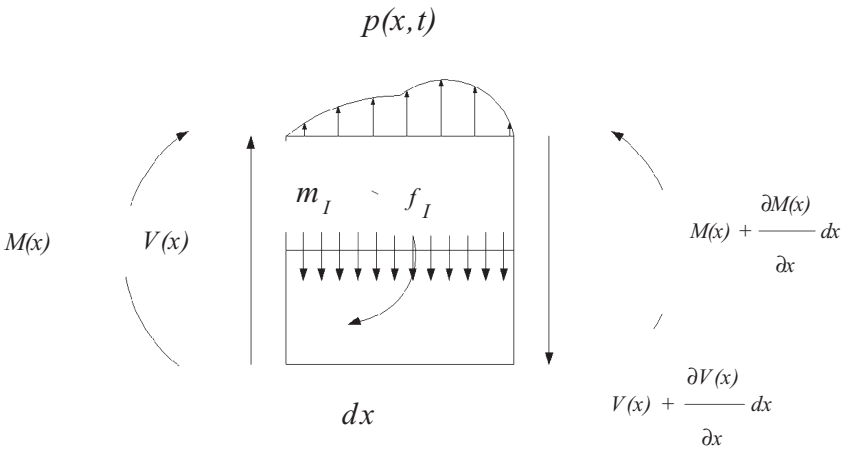

Figure 2. An element of the beam.

DOI: 10.1002/tal

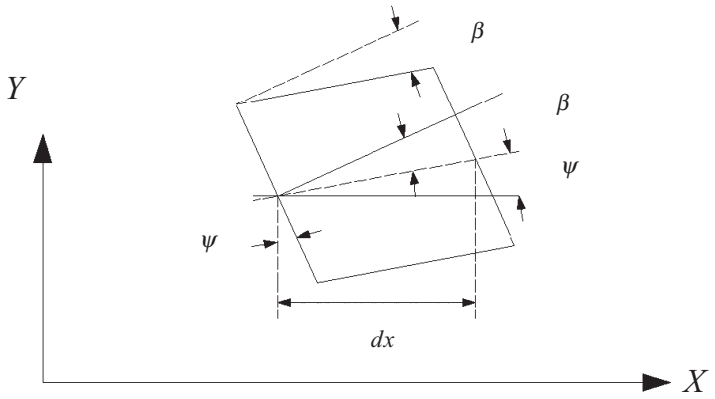

Figure 3. Components deformation of the beam.

When shear deformation and rotational moment of inertia are considered in the Timoshenko beam, the dynamic response analyses of structures with high slenderness ratio (L/r) are significantly affected. Figure 3 displays the beam's components of deformation. Rotational inertia is modelled using the rotated cross-sectional area of the beam rather than the initial vertical position ψ. If plan sections remain plane and perpendicular to the longitudinal axis after deformation, then ψ will be the slope of the beam's elastic curve.

A consequence of the assumption that plane section remaining plan after deformation is that the shear deformation β will cause a reduction in the slope of displacement curve as shown in Figure 3, thus:

$$\frac{\partial y}{\partial x} = \psi - \beta \tag{2}$$

Shear forces acting on cross-sectional area of the beam are related to rotation of elastic axis of the beam (β) as $V_{(x)} = k(x)A(x)G\beta$, where $k(x)A(x)$ is effective shear area of the section and the shear coefficient factor.

By using Equation (2), Equation (1) can be written as follows:

$$\frac{\partial}{\partial x}\left(k(x)GA(x)\left(\psi - \frac{\partial y}{\partial x}\right)\right) + m(x)\frac{\partial^2 y}{\partial t^2} = 0 \tag{3}$$

By applying rotational equilibrium to the element as shown in Figure 2, and by using curvature–moment relation $M(x) = EI(x)\dfrac{\partial \psi}{\partial x}$, one can obtain:

$$\frac{\partial}{\partial x}\left(EI(x)\frac{\partial \psi}{\partial x}\right) = k(x)GA(x)\left(\psi - \frac{\partial y}{\partial x}\right) + m_I(x) \tag{4}$$

Rotational inertia is defined as the product of mass moment of inertia and angular acceleration as follows:

$$m_I(x) = \rho(x)I(x)\frac{\partial^2 \psi}{\partial t^2} \tag{5}$$

In Equation (5), $I(x)$ is moment of inertia for the cross-sectional area, $\rho(x)$ is mass per unit volume. $\rho(x)$ can also can be written in terms of $r(x)$, beam's radius of gyration and $I(x)$ as follows:

$$\rho(x) = \frac{m(x)r(x)^2}{I(x)} \tag{5a}$$

DOI: 10.1002/tal

By using the earlier explained relation, and inserting in Equation (4), one can obtain:

$$\frac{\partial}{\partial x}\left(EI(x)\frac{\partial \psi}{\partial x}\right) = k(x)GA(x)\left(\psi - \frac{\partial y}{\partial x}\right) + m(x)r(x)^2\frac{\partial^2 \psi}{\partial t^2} \tag{6}$$

Equations (3) and (6) are simplified based on the assumption that flexural and shear rigidities along beam's height are constant, leading to:

$$kGA\frac{\partial}{\partial x}\left(\psi - \frac{\partial y}{\partial x}\right) + m\frac{\partial^2 y}{\partial t^2} = 0 \tag{7}$$

$$EI\frac{\partial}{\partial x}\left(\frac{\partial \psi}{\partial x}\right) = kGA\left(\psi - \frac{\partial y}{\partial x}\right) + mr^2\frac{\partial^2 \psi}{\partial t^2} \tag{8}$$

Omitting ψ from Equations (7) and (8) and combining them, the following equation is obtained:

$$EI\frac{\partial^4 y}{\partial x^4} + m\frac{\partial^2 y}{\partial t^2} - \frac{mEI}{kGA}\frac{\partial^2}{\partial x^2}\left(\frac{\partial^2 y}{\partial t^2}\right) - mr^2\frac{\partial^2}{\partial x^2}\left(\frac{\partial^2 y}{\partial t^2}\right) + \frac{m^2r^2}{kGA}\frac{\partial^4 y}{\partial t^4} = 0 \tag{9}$$

In Equation (9), the first two terms model vibration of the beam without considering the influence of shear deformation and rotational moment of inertia, which are modelled by the third and fourth terms, respectively, while the fifth term models the direct coupling between shear deformation and rotational inertia.

Using the method of separation of variables:

$$y_{(x,t)} = \varphi(x)e^{i\omega t} \tag{10}$$

In Equation (10), ω is the circular frequency and $\varphi(x)$ is the mode shape function.
Substituting Equation (10) into Equation (9) and dividing by $e^{i\omega t}$ yields:

$$EI\varphi(x)^{IV} + \omega^2\left(mr^2 + \frac{mEI}{A_sG}\right)\varphi(x)^{II} + \left(\frac{m^2\omega^4r^2}{A_sG} - m\omega^2\right)\varphi(x) = 0 \tag{11}$$

where $A_s = kA$. For the sake of clarity and simplicity, the following non-dimensional parameters are introduced:

$$a^2 = \frac{EI}{A_sGL^2} \tag{12}$$

$$b_n{}^2 = \frac{m\omega^2L^4}{EI} \tag{13}$$

$$R^2 = \left(\frac{r}{L}\right)^2 \tag{14}$$

$$\xi = \frac{x}{L} \Rightarrow \quad for \;\; 0 \le x \le L \quad then \quad 0 \le \xi \le 1 \tag{15}$$

thus:

$$\frac{d}{dx}\varphi(x) = \varphi(x)^{I} = \frac{d}{d\xi}(\varphi(\xi))\frac{d\xi}{dx} = \frac{1}{L}\varphi(\xi)^{I} \tag{16}$$

$$\frac{d^2}{dx^2}\varphi(x) = \varphi(x)^{II} = \frac{1}{L^2}\varphi(\xi)^{II} \tag{17}$$

DOI: 10.1002/tal

$$\frac{d^3}{dx^3}\varphi(x)=\varphi(x)^{\mathrm{III}}=\frac{1}{L^3}\varphi(\xi)^{\mathrm{III}} \tag{18}$$

$$\frac{d^4}{dx^4}\varphi(x)=\varphi(x)^{IV}=\frac{1}{L^4}\varphi(\xi)^{IV} \tag{19}$$

Substituting Equations (15–19) into Equation (11), the following equation is obtained:

$$\frac{EI}{L^4}\varphi(\xi)^{\mathrm{IV}}+\frac{\omega^2}{L^2}\left(mr^2+\frac{mEI}{A_sG}\right)\varphi(\xi)^{\mathrm{II}}+\left(\frac{m^2\omega^4r^2}{A_sG}-m\omega^2\right)\varphi(\xi)=0 \tag{20}$$

Substituting Equations (12–14) into Equation (20) and dividing by EI/L^4 leads to:

$$\varphi(\xi)^{IV}+b_n{}^2\left(R^2+a^2\right)\varphi(\xi)^{\mathrm{II}}+b_n{}^2\left(a^2R^2b_n{}^2-1\right)\varphi(\xi)=0 \tag{21}$$

In Equation (21), rotational moment of inertia may be neglected as explained in Section 3, which can be simplified as follows:

$$\varphi(\xi)^{IV}+b_n{}^2a^2\varphi(\xi)^{II}-b_n{}^2\varphi(\xi)=0 \tag{22}$$

Equation (22) is a fourth-order ordinary differential equation with constant coefficients. In these models, Equations (21) and (22), the coefficients a^2, R^2 and b_n^2 are greater than zero, thus $b_n^2(R^2+a^2)$ is greater than zero; however, coefficient $b_n^2(a^2R^2b_n^2-1)$ can have three states:
first state:

$$b_n{}^2\left(a^2R^2b_n{}^2-1\right)<0\Rightarrow\left(a^2R^2b_n{}^2-1\right)<0 \tag{23}$$

second state:

$$b_n{}^2\left(a^2R^2b_n{}^2-1\right)=0\Rightarrow\left(a^2R^2b_n{}^2-1\right)=0 \tag{24}$$

third state:

$$b_n{}^2\left(a^2R^2b_n{}^2-1\right)>0\Rightarrow\left(a^2R^2b_n{}^2-1\right)>0 \tag{25}$$

In the first state, by substituting Equations (12–14) into Equation (23), it yields:

$$0<\omega<A\sqrt{\frac{kG}{mI}} \tag{26}$$

In the second state, Equations (12–14) are substituted into Equation (24), leading to:

$$\omega=A\sqrt{\frac{kG}{mI}} \tag{27}$$

In the third state, by substituting Equations (12–14) into Equation (25), one gets:

$$\omega>A\sqrt{\frac{kG}{mI}} \tag{28}$$

In the first state, substituting $\varphi(\xi)=e^{d\xi}$ into Equation (21) leads to:

$$d^4+b_n{}^2\left(R^2+a^2\right)d^2+b_n{}^2\left(a^2R^2b_n{}^2-1\right)=0 \tag{29}$$

The roots of Equation (29) can be shown as follows:

$$d_{1,2}=\pm b \tag{30}$$

DOI: 10.1002/tal

$$d_{3,4} = \pm fi \tag{31}$$

where parameters S_1, S_2, b and f are defined as follows:

$$S_1 = -1 + \sqrt{1 - \frac{4\left(a^2 R^2 b_n{}^2 - 1\right)}{b_n{}^2\left(R^2 + a^2\right)^2}} > 0 \tag{32}$$

$$S_2 = -1 - \sqrt{1 - \frac{4\left(a^2 R^2 b_n{}^2 - 1\right)}{b_n{}^2\left(R^2 + a^2\right)^2}} < 0 \tag{33}$$

$$b = b_n \sqrt{\frac{\left(R^2 + a^2\right)}{2} S_1} \tag{34}$$

$$f = b_n \sqrt{-\frac{\left(R^2 + a^2\right)}{2} S_2} \tag{35}$$

and mode shape in the first state is:

$$\varphi(\xi) = A \sin h(b\xi) + B \cos h(b\xi) + C \sin(f\xi) + D \cos(f\xi) \tag{36}$$

In Equation (36), coefficients A, B, C and D for cantilevered beam model can be determined by applying the following boundary conditions:

$$\varphi(\xi = 0) = 0 \tag{37}$$

$$\varphi^{\mathrm{I}}(\xi = 0) = 0 \tag{38}$$

$$EI\varphi^{\mathrm{II}}(\xi = 1) = 0 \tag{39}$$

$$EI\varphi^{\mathrm{III}}(\xi = 1) - A_s G\varphi^{\mathrm{I}}(\xi = 1) = 0 \tag{40}$$

By substituting Equations (37–40) into Equation (36), an eigensystem is obtained, which is solved using Maple 10.0 (Waterloo Maple Inc., Waterloo, Canada).

The characteristic equation in the first state is obtained as follows:

$$\begin{aligned}&\left(b^4 + f^4\right)EI + A_s G\left(f^2 - b^2\right) + \left(bf\left(f^2 - b^2\right)EI + 2bfA_s G\right)\sin h(b)\sin(f) \\ &\quad + \left(2b^2 f^2 EI + A_s G\left(b^2 - f^2\right)\right)\cos h(b)\cos(f) = 0\end{aligned} \tag{41}$$

In the second state, by substituting $\varphi(\xi) = e^{d\xi}$ into Equation (21), it yields:

$$d^4 + b_n{}^2\left(R^2 + a^2\right)d^2 = 0 \tag{42}$$

Parameter f is defined as follows:

$$f = b_n \sqrt{\left(R^2 + a^2\right)} \tag{43}$$

thus the roots of Equation (42) are as follows:

$$d_{1,2} = 0 \tag{44}$$

$$d_{3,4} = \pm fi \tag{45}$$

DOI: 10.1002/tal

and mode shape for the second state is:

$$\varphi(\xi) = A + B\xi + C\sin(f\xi) + D\cos(f\xi) \tag{46}$$

In Equation (46), coefficients A, B, C and D are determined by applying the boundary conditions. Equations (37–40) are substituted into Equation (46); the characteristic equation in the second state is then obtained as follows:

$$f^2 EI + A_s G(1 - \cos(f)) = 0 \tag{47}$$

In the third state, substituting $\varphi(\xi) = e^{d\xi}$ into Equation (21) leads to:

$$d^2 = \frac{b_n{}^2\left(R^2 + a^2\right)}{2}\left(-1 \pm \sqrt{1 - \frac{4\left(a^2R^2b_n{}^2 - 1\right)}{b_n{}^2\left(R^2 + a^2\right)^2}}\right) \tag{48}$$

where

$$\left(a^2R^2b_n{}^2 - 1\right) > 0 \Rightarrow 1 - \frac{4\left(a^2R^2b_n{}^2 - 1\right)}{b_n{}^2\left(R^2 + a^2\right)^2} < 1 \tag{49}$$

In Equation (49), three states occur: state (a):

$$0 < 1 - \frac{4\left(a^2R^2b_n{}^2 - 1\right)}{b_n{}^2\left(R^2 + a^2\right)^2} < 1 \tag{50}$$

state (b):

$$1 - \frac{4\left(a^2R^2b_n{}^2 - 1\right)}{b_n{}^2\left(R^2 + a^2\right)^2} = 0 \tag{51}$$

state (c):

$$1 - \frac{4\left(a^2R^2b_n{}^2 - 1\right)}{b_n{}^2\left(R^2 + a^2\right)^2} < 0 \tag{52}$$

In state (a) parameters b and f are defined as follows:

$$b = b_n\sqrt{\frac{\left(R^2 + a^2\right)}{2}\left(1 - \sqrt{1 - \frac{4\left(a^2R^2b_n{}^2 - 1\right)}{b_n{}^2\left(R^2 + a^2\right)^2}}\right)} \tag{53}$$

$$f = b_n\sqrt{\frac{\left(R^2 + a^2\right)}{2}\left(1 + \sqrt{1 - \frac{4\left(a^2R^2b_n{}^2 - 1\right)}{b_n{}^2\left(R^2 + a^2\right)^2}}\right)} \tag{54}$$

thus, the roots of Equation (48) are as follows

$$d_{1,2} = \pm bi \tag{55}$$

$$d_{3,4} = \pm fi \tag{56}$$

and mode shape for state (a) is

$$\varphi(\xi) = A\sin(b\xi) + B\cos(b\xi) + C\sin(f\xi) + D\cos(f\xi) \tag{57}$$

DOI: 10.1002/tal

In Equation (57), coefficients A, B, C and D are determined by applying boundary conditions. Substituting Equations (37–40) into Equation (57), the characteristic equation for state (a) is obtained as follows:

$$\begin{aligned}&\left(b^4+f^4\right)EI+A_sG\left(f^2+b^2\right)-bf\left(b^2EI+2A_sG+f^2EI\right)\sin(f)\sin(b)\\&-\left(2b^2f^2EI+A_sG\left(b^2+f^2\right)\right)\cos(b)\cos(f)=0\end{aligned} \tag{58}$$

In state (b), parameter b is defined as follows

$$b=b_n\sqrt{\frac{\left(R^2+a^2\right)}{2}} \tag{59}$$

thus, the roots of Equation (48) are

$$d_{1,2}=bi \tag{60}$$

$$d_{3,4}=-bi \tag{61}$$

and the mode shape for state (b) is

$$\varphi(\xi)=A\sin(b\xi)+B\cos(b\xi)+C\xi\sin(b\xi)+D\xi\cos(b\xi) \tag{62}$$

In Equation (62), coefficients A, B, C and D are determined by applying the boundary conditions. Substituting Equations (37–40) into Equation (62), the characteristic equation in state (b) is obtained as follows:

$$b^4EI+b^2A_sG+3b^2EI+b^2EI\cos^2(b)+A_sG\sin^2(b)=0 \tag{63}$$

In state (c), parameters b, f and β are defined as follows:

$$b=b_n\sqrt{\frac{\left(R^2+a^2\right)}{2}}\sqrt[4]{\frac{4\left(a^2R^2b_n{}^2-1\right)}{b_n{}^2\left(R^2+a^2\right)^2}}\cos\left(\frac{\arctan(\beta)}{2}\right) \tag{64}$$

$$f=b_n\sqrt{\frac{\left(R^2+a^2\right)}{2}}\sqrt[4]{\frac{4\left(a^2R^2b_n{}^2-1\right)}{b_n{}^2\left(R^2+a^2\right)^2}}\sin\left(\frac{\arctan(\beta)}{2}\right) \tag{65}$$

$$\beta=\sqrt{\frac{4\left(a^2R^2b_n{}^2-1\right)}{b_n{}^2\left(R^2+a^2\right)^2}-1} \tag{66}$$

Thus, the roots of Equation (48) are

$$d_{1,2}=b\pm fi \tag{67}$$

$$d_{3,4}=-b\pm fi \tag{68}$$

and the mode shape for state (c) is

$$\varphi(\xi)=e^{b\xi}\left(A\sin(f\xi)+B\cos(f\xi)\right)+e^{-b\xi}\left(C\sin(f\xi)+D\cos(f\xi)\right) \tag{69}$$

In Equation (69), coefficients A, B, C and D are determined by applying the boundary conditions. Substituting Equations (37–40) into Equation (69), the characteristic equation for state (b) becomes:

DOI: 10.1002/tal

$$\begin{aligned}&\left(e^{b}\right)^{2}\left[-b^{2}f^{2}A_{s}G-f^{6}EI-f^{4}A_{s}G-6b^{4}f^{2}EI\cos^{2}(f)-b^{4}f^{2}EI\right.\\&+4f^{4}b^{2}EI\cos^{2}(f)-2b^{2}f^{4}EI\sin^{2}(f)-3b^{5}fEI\sin(f)\cos(f)+6f^{3}b^{3}EI\sin(f)\cos(f)\\&\left.-3bf^{5}EI\sin(f)\cos(f)\right]+(e^{-b})^{2}\left[-b^{4}f^{2}EI-f^{6}EI-f^{4}A_{s}G-2f^{4}b^{2}EI\right.\\&\left.-b^{2}f^{2}A_{s}G\right]+\left(e^{b}\right)\left(e^{-b}\right)\left[2f^{4}A_{s}G+2f^{6}EI+2b^{2}f^{2}A_{s}G\cos(2f)-6b^{2}f^{4}EI\right.\\&-2b^{2}f^{4}EI\sin^{2}(f)-6b^{4}f^{2}EI-14b^{4}f^{2}EI\cos^{2}(f)+4b^{6}EI\sin^{2}(f)\\&\left.+3b^{5}fEI\sin(f)\cos(f)-6b^{3}f^{3}EI\sin(f)\cos(f)+3f^{5}bEI\sin(f)\cos(f)\right]=0\end{aligned}\tag{70}$$

In Equation (22), the R^2 parameter is neglected and by substituting $\varphi(\xi) = e^{d\xi}$, it can be simplified to

$$d^{2}=\frac{b_{n}{}^{2}a^{2}}{2}\left(-1\pm\sqrt{1+\frac{4}{b_{n}{}^{2}a^{4}}}\right)\tag{71}$$

since

$$-1+\sqrt{1+\frac{4}{b_{n}{}^{2}a^{4}}}>0\tag{72}$$

and

$$-1-\sqrt{1+\frac{4}{b_{n}{}^{2}a^{4}}}<0\tag{73}$$

Parameters b and f are defined as follows:

$$b=\frac{ab_{n}}{\sqrt{2}}\sqrt{-1+\sqrt{1+\frac{4}{b_{n}{}^{2}a^{4}}}}\tag{74}$$

$$f=\frac{ab_{n}}{\sqrt{2}}\sqrt{1+\sqrt{1+\frac{4}{b_{n}{}^{2}a^{4}}}}\tag{75}$$

Roots of Equation (71) are obtained as follows:

$$d_{1,2}=\pm b\tag{76}$$

$$d_{3,4}=\pm fi\tag{77}$$

thus, the mode shape is

$$\varphi(\xi)=A\sin h(b\xi)+B\cos h(b\xi)+C\sin(f\xi)+D\cos(f\xi)\tag{78}$$

In Equation (78), coefficients A, B, C and D are determined by applying the boundary conditions. Substituting Equations (37–40) into Equation (78), the characteristic equation for state (b) is obtained as follows:

$$\begin{aligned}&\left(b^{4}+f^{4}\right)EI+A_{s}G\left(f^{2}-b^{2}\right)+\left(bf\left(f^{2}-b^{2}\right)EI+2bfA_{s}G\right)\sin h(b)\sin(f)\\&+\left(2b^{2}f^{2}EI+A_{s}G\left(b^{2}-f^{2}\right)\right)\cos h(b)\cos(f)=0\end{aligned}\tag{79}$$

3. SENSITIVITY OF R^2

In Equation (29), coefficient R^2 is reciprocal of the square of slenderness ratio. When the slenderness ratio is one (the height of building is equal to gyration radius), so far, coefficient R^2 is equal to unit, but for values of slenderness ratio larger than one (the height of building is larger than gyration radius), coefficient R^2 is very small (as has been shown in example in this paper) because coefficient R^2 is

DOI: 10.1002/tal

reciprocal of the square of slenderness ratio. For values of slenderness ratio smaller than one (the height of building is smaller than gyration radius), the coefficient R^2 is very large and so far can not be neglected. So far, one is an acceptable number between two domains of large and small values of slenderness ratio because for values smaller than one, the square of these values are very small, and so far, reciprocal of them are very large, and so far, coefficients R^2 are very large and vice versa for values larger than one.

For small values of (L/r), the coefficient R^2 has a large value and can not be neglected. Therefore, Equation (21) is suitable for small values of (L/r), but for large value of (L/r), the coefficient R^2 is small and can be neglect. In this case, Equation (22) is suitable. For simplicity, it has been assumed that the cross-sectional area is rectangular (but this conclusion is valid for all types of sections). In the rectangular section that is shown in Figure 4, slenderness ratio can be fined by the following relationship:

$$\frac{L}{r} = \frac{L}{\sqrt{\frac{L_f L_w^3}{12 L_f L_w}}} = \frac{\sqrt{12}L}{L_w} \tag{80}$$

where L is the total height of a given tall building and L_w is the length of web panel.

Equation (80) shows that the slenderness ratio is related to the total building height and length of the web panel. It has been assumed that L_w is constant and L varies. Figure 5 shows the height of a tall building with respect to slenderness ratio for a different value of L. This diagram is linear, but if it was assumed that L is constant and L_w is varying, then for this state, the slenderness ratio would vary exponentially with respect to web's length L_w. In both of the two states, a critical length can be obtained when the slenderness ratio is one.

Referring to Figure 5, if the height of a given tall building is greater than its critical length (L_{cr}), we can neglect the effects of R^2; hence, in this state, Equation (22) can be used. If height is smaller than L_{cr}, then R^2 can not be neglected and Equation (21) must be used for this state.

It should be noted that in cases where L/r is small, the effect of R^2 becomes significant and one has to use Equation (21), which is defined over the eigen spectum of the first five natural frequencies; hence, five eigen functions are needed to be determined. However, if L/r is larger, then R^2 may be neglected and only one eigen function must be evaluated using Equation (22).

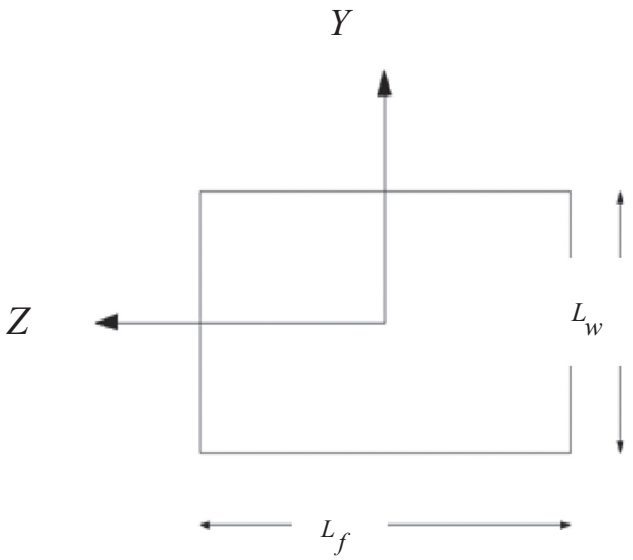

Figure 4. Rectangular section.

DOI: 10.1002/tal

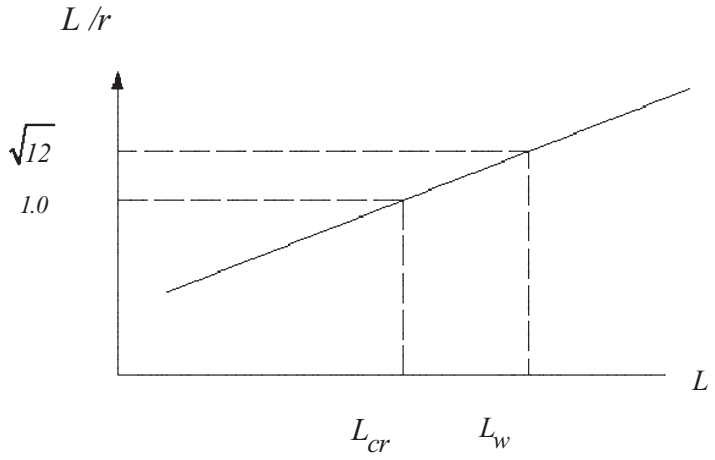

Figure 5. Relationship between slenderness ratio and height of tall buildings.

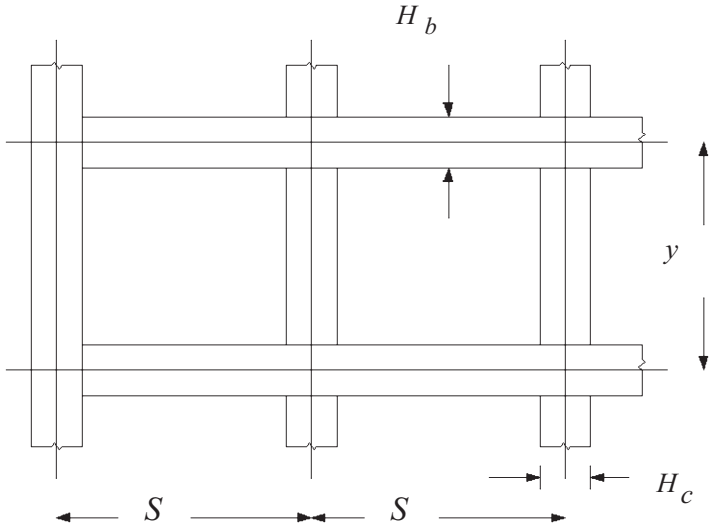

Figure 6. Typical elevation of framed tube structure.

4. MASS PER UNIT HEIGHT OF FRAMED TUBE STRUCTURE

In this paper, it is assumed that sections of beams and columns are equal in both web and flange panels along the height, that the size of beams and columns are equal and that the distance from centre to centre for columns in both web and flange panels is equal. Denoting the centre to centre distance for columns by S, the width and depth for beams with B_b and H_b, respectively, and for columns with B_c and H_c, it is assumed that $B_b = B_c$ and $H_b = H_c$; cross-sectional area of the beam is shown using A_b, cross-sectional area of column with A_c, hence, $A_b = A_c$. Number of stories in the building is denoted by n, slab thickness with t_s, mass per unit volume of the materials with ρ, total building height by L, and based on Figures 6 and 7, one obtains:

$$W_b = \left[2A_b\left(L_f - H_b\right) + 2A_b\left(L_w - H_b\right)\right]n\rho \tag{81}$$

DOI: 10.1002/tal

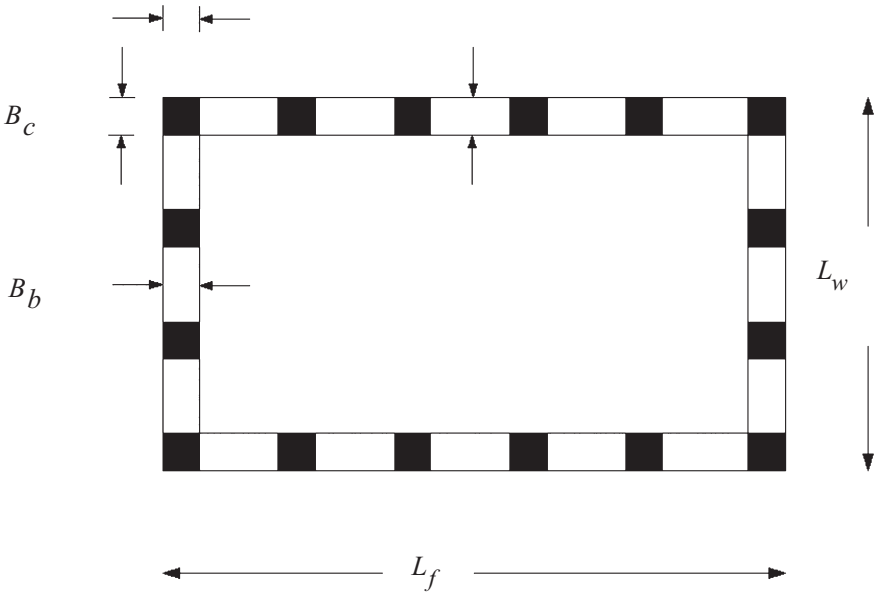

Figure 7. Typical plan of framed tube structures.

$$W_c = \left[2A_c(y-H_b)\rho\left(\frac{L_f}{S}-1\right)\right]n + \left[2A_c(y-H_b)\rho\left(\frac{L_w}{S}-1\right)\right]n + \left[4LH_b^2\rho\right] + \left[4L(H_c-H_b)^2\rho\right] \tag{82}$$

$$W_s = \left[\left[(L_f-H_b)(L_w-H_b)\right] - \left[4(H_c-H_b)^2\right]\right]t_s\rho n \tag{83}$$

$$m = \frac{W_b + W_c + W_s}{L} \tag{84}$$

where y is the distance from centre to centre of stories, W_c is total mass of the columns, W_b is total mass of the beams, W_s is total mass of the slabs, L_f is length of the flange panel, m is mass per unit height of the tall building and L_w is length of the web panel.

5. GEOMETRICAL PROPERTIES OF SECTIONS

The method that is being used by the writers has been given in the Appendix, which is actually an abridged version of Ha *et al*.'s method. This method is less sophisticated than Ha *et al*.'s original method and is thus simpler to apply. On the other hand, since the shear deformations of the frame members are taken into account, it is more accurate than Coull and Bose's method (Kwan, 1994).

Considering Figure 8, the equivalent cross-sectional area of plan of a framed tube structure is:

$$A = (L_f L_w) - (L_f - 2t)(L_w - 2t) \tag{85}$$

In Equation (85), higher power terms of t are neglected due to smallness of t, thus:

$$A = 2t(L_f + L_w) \tag{86}$$

DOI: 10.1002/tal

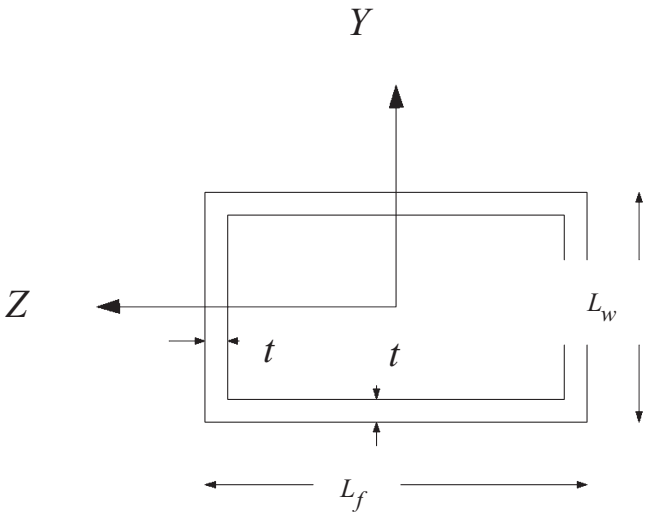

Figure 8. Computing of geometrical properties of section.

The moment of inertia of the plan for rotational vibration about the z-axis is:

$$I_z = \frac{1}{12} L_f L_w^3 - \frac{1}{12}(L_f - 2t)(L_w - 2t)^3 \tag{87}$$

Again, ignoring higher powers of t yields,

$$I_z = \frac{1}{2} L_f L_w^2 t + \frac{1}{6} L_w^3 t \tag{88}$$

6. SHEAR COEFFICIENT FACTOR

One of the most accurate beam vibration models is based on Timoshenko's theory, which was given in the spectral form earlier. The only thing left to discuss is the shape factor or shear coefficient factor k. According to the commonly accepted definition, shape factor k is the ratio of the average shear strain on a section to the shear strain at the centroid depend only the shape of the beam cross-section (Bathe, 1982). However, there is strong evidence that the accepted definition of k leads to unsatisfactory results for the high-frequency spectrum (Horr and Schmidt, 1995). The problem arises when the distribution of shear strain over a cross-section depends on the mode of vibration of the beam. Using static strain distribution to calculate the shape factor causes a considerable error in calculation. The shear coefficient factor k, used in equations of motion, is introduced to account for the fact that the shear stress and shear strain are not uniformly distributed over the cross-section. Cowper (1966) suggested methods based upon the three-dimensional elasticity to calculate the shear coefficient as a function of the shape of the cross-section and of Poisson's ratio. Stephen (1978) showed variation in the shear coefficient with frequency, but this dependence seems to be of slight importance. Shear coefficients for Timoshenko's beam theory for various cross-sections is given by (Hutchinson, 2001)

$$k = -\frac{2(1+\nu)}{\left[\frac{A}{I_z^2} C_4 + \nu\left(1 - \frac{I_y}{I_z}\right)\right]} \tag{89}$$

DOI: 10.1002/tal

where v is the Poisson's ratio and I_z and I_y are the moments of inertia about the z-axis and y-axis, respectively, and coefficient C_4 is defined as follows:

$$C_4 = -\int_A \left[v\left(f_1 y^2 - f_1 z^2 + 2 f_2 yz\right) + 2(1+v)\left(f_1^2 + f_2^2\right)\right] dA \tag{90}$$

where the functions f_1 and f_2, defined earlier are the in-plane distribution of the shearing stresses τ_{xy} and τ_{xz}. These functions are defined as follows:

$$\tau_{xy} = \frac{V}{I_z} f_1(y, z) \tag{91}$$

$$\tau_{xy} = \frac{V}{I_z} f_2(y, z) \tag{92}$$

Hutchinson with the aforementioned expression calculates coefficient k for various cross-sections. For instance, in a rectangular cross-section, k is defined as follows:

$$k = -\frac{2(1+v)}{\left[\frac{9}{4a^5 b} C_4 + v\left(1 - \frac{b^2}{a^2}\right)\right]} \tag{93}$$

$$C_4 = \frac{4}{45} a^3 b\left(-12a^2 - 15va^2 + 5vb^2\right) + \sum_{n=1}^{\infty} \frac{16v^2 b^5 \left(n\pi a - b\tanh\left(\frac{n\pi a}{b}\right)\right)}{(n\pi)^5 (1+v)} \tag{94}$$

where the depth of the beam (y-direction) is $2a$ and the width of the beam (z-direction) is $2b$.

With several numerical examples, this fact was recovered that k factor increases with the number of series term and with attention to other k factors for other sections, it was seen that k factor may vary 0.85 to 0.95. In this paper, k factor has assumed to be one.

7. ACCURACY OF THE RESULTS

To illustrate the accuracy of the proposed method, a simple symmetrical framed tube structure is studied. A high-rise 40-storey reinforced concrete framed tube structure is considered. All the beam and column members are of sizes 0.8 × 0.8 m. The height of each storey is 3.0 m and the centre-to-centre spacing of columns is 2.5 m. The Young's and shear modulus of the material are 20.4×10^8 kg/m^2 and 81.6×10^7 kg/m^2, respectively, the mass per unit volume of the material is 2400 kg/m^3. The equivalent elastic properties of the analogous orthotropic membrane tube as evaluated by the relationships that are given in the paper and in the Appendix are as follows:

$E = E_m = 20.4 \times 10^8\ kg/m^2$, $G_m = 81.6 \times 10^7\ kg/m^7$, $t = 0.256\ m$
$L_f = 35\ m$, $L_w = 30\ m$, $B_b = B_c = H_b = H_c = 0.8\ m$, $S = 2.5\ m$
$\rho = 2400\ kg/m^3$, $K = 1$, $A_b = A_c = 0.64\ m^2$, $I_b = I_c = 3.413 \times 10^{-2}\ m^4$
$A = 33.28\ m^3$, $A_s = 33.28\ m^2$, $t_s = 0.3\ m$, $L = 120\ m$,
$W_b = 7.79 \times 10^6\ kg$, $W_c = 7.22 \times 10^6\ kg$, $W_s = 2.88 \times 10^7\ kg$, $m = 3.65 \times 10^5\ kg/m$,
$I_z = 5184\ m^4$, $\Delta_b/Q = 1.69 \times 10^{-8}\ m/kg$, $\Delta_s/Q = 8.902 \times 10^{-9}\ m/kg$,
$G = 17.61 \times 10^7\ kg/m$, $r = \sqrt{I/A} = 12.48\ m$, $\frac{L}{r} = 9.615$, $R^2 = (r/L)^2 = 1.08 \times 10^{-2}$

By computing parameters f, b, EI and AsG and inserting in Equations (41) or (79) (because the value of coefficient R^2 is small and can be neglected) and by writing a computational program in MATLAB (Version 7.9.0.529 Mathworks Inc., California, USA, 2009) or in other mathematical computational packages, we can obtain first root of characteristic equation that this root is first natural frequency of the mentioned structure.

DOI: 10.1002/tal

By inserting these data into Equations (41) or (79) through an iterative numerical process, natural frequency can be obtained as $\omega_1 = 1.42$ rad/s. The value of ω_1 by finite element method is $\omega_1 = 1.53$ rad/s. The proposed approximate method underestimates the natural frequency by 7%. The proposed method shows a good understanding of structural behaviour, easy to use, yet reasonably accurate and suitable for quick evaluations during the preliminary design stage, which requires less time. The main sources of error between the proposed approximate method and the finite element method are as follows:

- all closely spaced perimeter columns tied at each floor level by deep spandrel beams are considered to form a tubular structure;
- effect of shear lag phenomenon along height of tall building has been neglected;
- equivalencing the elastic properties of the framed tube such as G.

8. CONCLUSION

The formulae proposed in this paper can be used as an alternative to determine the natural frequency of framed tube structures. The numerical example shows that the approximate value of natural frequency obtained by the proposed method appears to be 7% smaller than the more accurate finite element method results. From the point of view of a structural engineer, this error is within the acceptable range of engineering practice, and therefore, the proposed method may be used to estimate the natural frequency at the preliminary stages in a structural design, which requires less time.

REFERENCES

Bathe KJ. 1982. *Finite Element Procedure in Engineering Analysis*. Prentice-Hall: Englewood Cliffs, NJ.

Cowper GR. 1966. The shear coefficient in Timoshenko's beam theory. *Journal of Applied Mechanics* **33**: 335–340.

Dym CL, Williams HE. 2007. Estimating fundamental frequencies of tall buildings. *ASCE Journal of Structural Engineering* **133**(10): 1–5.

Fung EHK, Yau DTW. 2001. Vibration frequencies of a rotating flexible arm carrying a moving mass. *Journal of Sound and Vibration* **241**(5): 857–878.

Horr AM, Schmidt LC. 1995. Closed form solution for the Timoshenko theory using a computer based mathematical package. *International Journal of Computers and Structures* **55**(3): 405–412.

Hutchinson JR. 2001. Shear coefficients for Timoshenko beam theory. *ASME Journal of Applied Mechanics* **68**: 87–92.

Kaviani P, Rahgozar R, Saffari H. 2008. Approximate analysis of tall buildings using sandwich beam models with variable cross-section. *Structural Design of Tall and Special Buildings* **17**: 401–418.

Kuang JS, Ng SC. 2004. Coupled vibration of tall buildings structures. *Structural Design of Tall and Special Buildings* **13**: 291–303.

Kuang JS, Ng SC. 2009. Lateral shear St. Venant torsion coupled vibration of asymmetric-plan frame structures. *Structural Design of Tall and Special Buildings* **18**(6): 647–656.

Kwan AKH. 1994. Simple method for approximate analysis of framed tube structures. *ASCE Journal of Structural Engineering* **120**(4): 1221–1239.

Lee WH. 2007. Free vibration analysis for tube-in-tube tall buildings. *Journal of Sound and Vibration* **303**: 287–304.

Li QS, Fang JQ, Jeary AP. 2002. Free vibration analysis of cantilevered tall structures under various axial loads. *Journal of Engineering Structures* **22**: 525–534.

Stephen N. 1978. On the variation of Timoshenko's shear coefficient with frequency. *Journal of Applied Mechanics* **45**: 695–700.

Swaddiwudhipong S, Soelarno Sidji S, Lee SL. 2002. The effects of axial deformation and axial force on vibration characteristics of tall buildings. *Structural Design of Tall and Special Buildings* **11**: 309–328.

Wang Q. 1996a. Sturm–Liouville equation for free vibration of a tube-in-tube tall building. *Journal of Sound and Vibration* **191**(3): 349–355.

Wang Q. 1996b. Modified ODE-solver for vibration of tube-in-tube structures. *Computer Methods in Applied Mechanics and Engineering* **129**: 151–156.

Yavari A, Sarkani S, Moyer ET Jr. 2000. On applications of generalized functions to beam bending problems. *International Journal of Solids and Structures* **37**(40): 5675–5705.

DOI: 10.1002/tal

APPENDIX: GEOMETRICAL PROPERTIES OF SECTIONS

As mentioned by Kwan (1994) a typical frame segment bounded by centers of adjacent frame members (columns and beams), Figure 9, constitute a basic unit of the frame and may be modeled as a solid membrane such that the elastic properties of the membrane would model the axial and shear behavior of the actual framework. The method for evaluating equivalent properties of a membrane is presented in next. This method is applicable to both the web and flange panels, and thus in the followings, they are not distinguished from each other.

AXIAL STIFFNESS

Under the action of vertical axial forces, the load-deformation relationships for both the frame unit and the equivalent membrane will be equal if

$$ESt = E_m A_c \tag{95}$$

where E is equivalent elastic modulus of the membrane, t is the thickness of the membrane and E_m is the elastic modulus of the construction materials. It is common practice to fix the value of t such that the area of the membrane is equal to the cross sectional area of the column (i.e. $St = A_c$) and so that the axial stress in the column and that in the membrane are equal. In such a case:

$$t = \frac{A_c}{S} \tag{96}$$

and

$$E = E_m \tag{97}$$

SHEAR STIFFNESS

Now consider the case of a frame unit subjected to a lateral force Q (Figure 10). The lateral deflection may be computed as the sum of that due to bending Δ_b and due to shear Δ_s. The bending deflection Δ_b is given by:

$$\frac{\Delta_b}{Q} = \frac{(y - H_b)^3}{12E_m I_c} + \left(\frac{y}{S}\right)^2 \frac{(S - H_c)^2}{12E_m I_b} \tag{98}$$

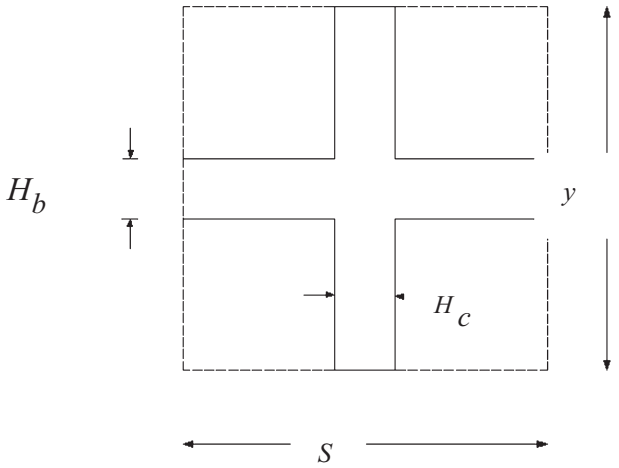

Figure 9. Membrane analogy for basic frame unit equivalent membrane.

DOI: 10.1002/tal

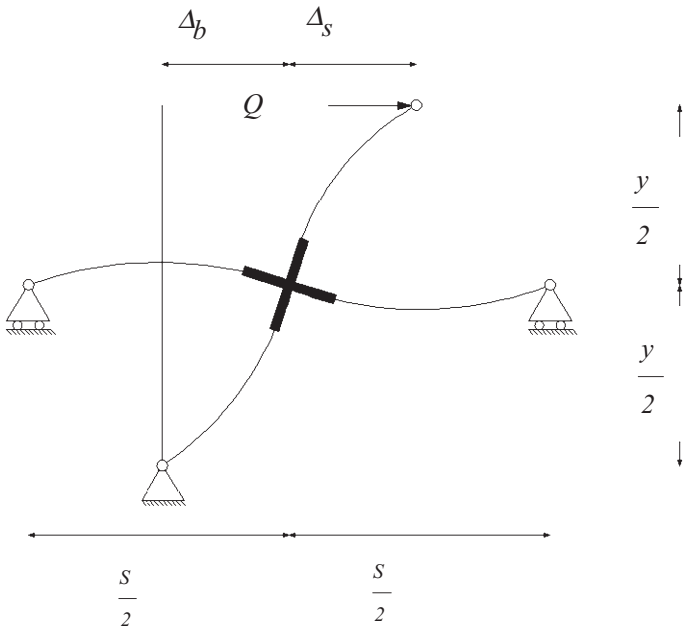

Figure 10. Basic frame unit under lateral shear force.

where I_b and I_c are moments of inertia of the beam and column, respectively. On the other hand, the shear deformation Δ_s is given by:

$$\frac{\Delta_s}{Q} = \frac{(y - H_b)}{G_m A_{sc}} + \left(\frac{y}{S}\right)^2 \frac{(S - H_c)}{G_m I_{sb}} \tag{99}$$

$$A_{sc} = kA_c \tag{100}$$

$$A_{sb} = kA_b \tag{101}$$

In which A_{sb} and A_{sc} are effective shear area of the beam and column, respectively, and G_m is shear modulus of the materials. Equating total lateral deflection of the frame unit to shear deflection of the membrane, the following equation is obtained:

$$\Delta_b + \Delta_s = Q \frac{y}{GSt} \tag{102}$$

where G is the equivalent shear modulus for membrane. From this equation, the value of G is derived as:

$$G = \frac{\frac{y}{St}}{\frac{\Delta_b}{Q} + \frac{\Delta_s}{Q}} \tag{103}$$

In which $\frac{\Delta_b}{Q}$ and $\frac{\Delta_s}{Q}$ are as given by Equations (98) and (99), respectively.

DOI: 10.1002/tal